Journal of Power and Energy Engineering, 2026, 14(11), 52-67
https://www.scirp.org/journal/jpee
ISSN Online: 2327-5901
ISSN Print: 2327-588X

Design and Experimental Performance Evaluation of an Autonomous Solar Panel Cleaning Robot

Mohd Rusdy Yaacob*, Anuar Mohamed Kassim, Nik Nurqairina Eriza Nik Ahmad Yusri

Fakulti Teknologi dan Kejuruteraan Elektrik, Universiti Teknikal Malaysia Melaka, Melaka, Malaysia
Email: *rusdy@utem.edu.my

How to cite this paper: Yaacob, M.R., Kassim, A.M. and Yusri, N.N.E.N.A. (2026) Design and Experimental Performance Evaluation of an Autonomous Solar Panel Cleaning Robot. *Journal of Power and Energy Engineering*, **14**, 52-67.
https://doi.org/10.4236/jpee.2026.1411004

Received: October 2, 2026
Accepted: November 10, 2026
Published: November 13, 2026

Copyright © 2026 by author(s) and Scientific Research Publishing Inc.
This work is licensed under the Creative Commons Attribution International License (CC BY 4.0).
http://creativecommons.org/licenses/by/4.0/

Open Access

Abstract

The growing deployment of solar photovoltaic (PV) systems has increased the need for reliable and sustainable maintenance solutions to mitigate performance losses caused by surface soiling. This study presents the design, development, and experimental evaluation of an autonomous water-free solar panel cleaning robot integrating an ESP32-based control system, edge detection, a mechanical brush-and-blower cleaning mechanism, and interchangeable locomotion modules. Three comparative experiments were conducted to evaluate key design choices. Infrared and ultrasonic sensors were compared for panel-edge detection; forward-rotating and plane-rotating brushes were evaluated for cleaning coverage; and wheel-based and track-based drivetrains were tested on inclined surfaces. The infrared sensor achieved 100% detection accuracy with a mean motion-to-detection time of 5.09 s, compared with 71.43% accuracy for the ultrasonic sensor. The plane-rotating brush achieved 75.0% mean cleaning coverage, 25.0% residue, and a coefficient of variation of 4.8%. The track-based drivetrain maintained stable mean traversal times from 5.44 s at 0˚ to 5.97 s at 9˚, with low run-to-run variability. These results provided a data-driven basis for integrating the infrared sensor, plane-rotating brush with blower, and track-based drivetrain into the final prototype. The study demonstrates proof-of-concept feasibility for compact autonomous and water-free PV maintenance under controlled experimental conditions.

Keywords

Solar Panel Cleaning Robot, Photovoltaic, Autonomous Robot, Dry Cleaning, Track-Based Locomotion

1. Introduction

Solar photovoltaic (PV) technology has become an increasingly important component of renewable energy generation due to its clean operation, scalability, and declining implementation costs. However, maintaining the expected energy yield of PV installations requires consideration of environmental factors that influence module performance. Among these factors, surface soiling is particularly important because deposited dust, dirt, and other airborne contaminants reduce the solar irradiance reaching photovoltaic cells and consequently decrease electrical output [1]. The severity of soiling is influenced by local dust characteristics, humidity, wind, rainfall, panel inclination, and other environmental conditions [2]. Previous studies have demonstrated that the effects of dust extend beyond optical transmittance and can influence the electrical and thermal performance of PV modules [3]. Consequently, cleaning and soiling mitigation remain important aspects of PV system operation and maintenance [4].

Several methods have been developed to mitigate PV soiling, ranging from conventional manual and water-based cleaning to mechanical, electrostatic, coating-based, and automated approaches [5]. Although water-assisted cleaning can effectively remove strongly adhered contaminants, repeated cleaning requires water resources and additional maintenance infrastructure. Water-free alternatives are therefore attractive, particularly for locations where water availability is limited. Electrostatic systems, for example, have demonstrated the ability to remove deposited particles without conventional washing [6], while automated dry-brushing systems have been successfully evaluated for long-term robotic PV maintenance [7]. Robotic cleaning has also been investigated for rooftop PV installations as a means of reducing repetitive manual intervention [8].

Autonomous cleaning robots provide an alternative approach by combining mechanical cleaning with embedded sensing and controlled locomotion. Antonelli *et al.* [9] developed a waterless autonomous robot incorporating helical brushes and ultrasonic positioning for PV panels in desert environments. Salman *et al.* [10] demonstrated a portable robotic dry cleaner using an ESP32 controller and automated monitoring, while Mousavi and Farahani [11] introduced a suction-based robot incorporating brushes and ultrasonic localization. Dry-cleaning robots incorporating visual assessment of panel soiling have also been investigated [12]. Reviews of solar-panel cleaning robots indicate that the effectiveness of such systems depends on the combined performance of cleaning, locomotion, sensing, control, and navigation subsystems [13].

Locomotion and navigation are particularly important because PV panels are commonly installed at an inclination, requiring sufficient traction and stable movement. Yang *et al.* [14] showed that increasing the contact area of the locomotion mechanism can improve traction in photovoltaic cleaning applications. Automated monitoring and control have also been combined with IoT-based cleaning systems [15], while Kim *et al.* [16] demonstrated localization of a self-driving cleaning ro-

bot using vision processing, wheel encoder information, and sensor fusion. Path-planning approaches have further been investigated to improve systematic panel coverage [17]. Other automated cleaning systems have emphasized mechanical simplicity and repeatable cleaning operation [18].

Apart from technical performance, cleaning frequency and operating strategy affect the overall feasibility of PV maintenance. Investigations under semi-arid conditions have shown that appropriate cleaning schedules need to balance energy recovery with cleaning and operating costs, and robotic cleaning can potentially reduce maintenance expenditure [19]. Similarly, optimum cleaning intervals depend strongly on local soiling conditions, panel inclination, and economic considerations [20]. These findings reinforce the need for cleaning systems that are not only effective in removing dust but are also reliable, repeatable, and capable of autonomous operation.

Despite the development of numerous photovoltaic cleaning systems, limited experimental work directly compares alternative sensor technologies, brush configurations, and drivetrain arrangements under the same lightweight robotic platform and controlled operating conditions. Many previous studies concentrate on the performance of a complete robot rather than experimentally evaluating competing subsystem configurations before final integration [9]-[13]. Consequently, the relative influence of sensing reliability, brush geometry, and drivetrain configuration on the performance of a compact autonomous cleaning robot remains an important design consideration.

Accordingly, this study presents the design, development, and experimental evaluation of an autonomous solar panel cleaning robot using a dry-cleaning mechanism and an ESP32-based control system. Three comparative experiments were conducted. Infrared and ultrasonic sensors were first evaluated for panel-edge detection. Forward-rotating and plane-rotating brush configurations were subsequently compared in terms of cleaning coverage and consistency. Finally, wheel-based and track-based drivetrains were evaluated over different panel inclinations. The experimental results were then used to select and integrate the sensing, cleaning, and locomotion subsystems into the final prototype.

2. Methodology

The autonomous solar panel cleaning robot was developed through an integrated design-and-evaluation approach involving mechanical construction, hardware integration, embedded control, and comparative experimental testing. The system was designed to perform dry mechanical cleaning while autonomously navigating a photovoltaic panel surface. An ESP32 microcontroller coordinated the locomotion, edge-detection, and cleaning subsystems. Three controlled experiments were subsequently conducted to compare alternative components for edge detection, cleaning coverage, and inclined locomotion before the final configuration was selected. All experimental conditions were repeated seven times to provide comparable performance measurements.

2.1. Prototype Design and Hardware Integration

The robot was developed as a compact water-free cleaning platform. Mechanical brushing was selected because previous studies have demonstrated its suitability for automated PV cleaning while avoiding continuous water consumption [5] [7] [9] [12]. Track-based and wheel-based locomotion were incorporated as interchangeable configurations because traction and contact characteristics can significantly affect robotic movement on inclined surfaces [13] [14]. Infrared and ultrasonic sensing were considered for edge detection because these sensing approaches have been employed in autonomous PV cleaning platforms [9]-[11] [16]. The overall system architecture and interconnection between the power supply, sensing, control, locomotion, and cleaning subsystems are shown in Figure 1.

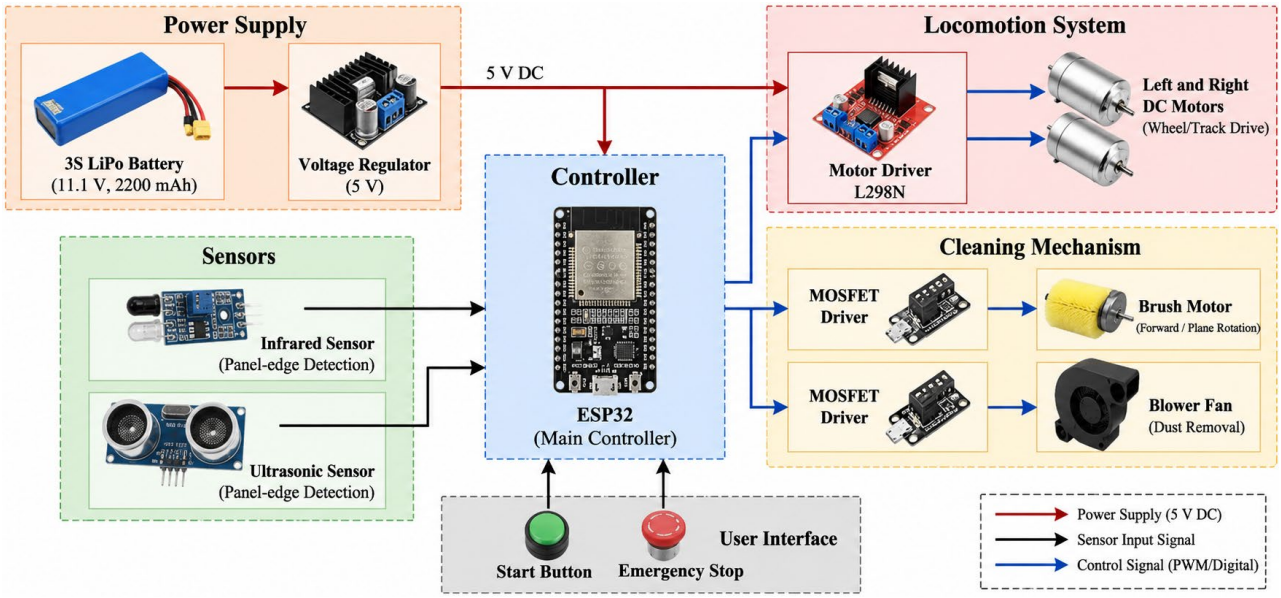


Figure 1. Block diagram of the autonomous solar panel cleaning robot.

The chassis was fabricated using PETG through 3D printing. The rectangular base measured approximately 220 mm × 180 mm × 60 mm, with a 2 mm wall thickness, 20% gyroid infill, and a 0.2 mm printing layer height. Interchangeable side mounting points allowed either wheel-based or track-based drivetrain configurations to be installed. The open-top structure provided access to the electronic components, while the low centre of gravity was intended to improve stability during inclined traversal. The completed prototype and arrangement of the major hardware components are shown in Figure 2.

An ESP32 development board was used as the main controller, supported by an L298N dual H-bridge motor driver. ESP32-based control and monitoring have also been applied in previous automated PV cleaning systems because the platform combines embedded processing with integrated wireless communication [10] [15]. Electrical power was supplied by a 3S lithium-polymer battery rated at

11.1 V and 2200 mAh, with an LM2596 DC-DC buck converter for voltage regulation. The cleaning subsystem employed a TT DC geared motor, interchangeable cylindrical and circular brushes, and a 6 V blower fan. The brush motor was switched through an IRLZ44N logic-level MOSFET with a flyback diode for protection. The main hardware components and their specifications are summarized in Table 1.

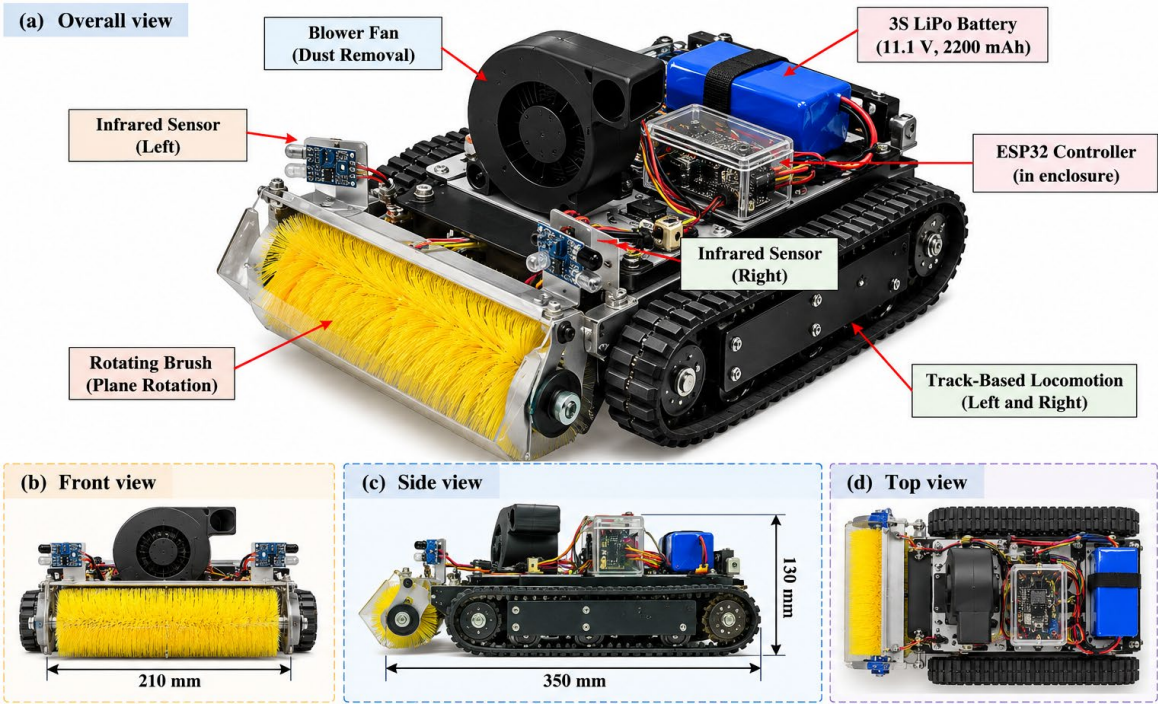


Figure 2. Developed autonomous solar panel cleaning robot and major hardware components.

Table 1. Main hardware components of the prototype.

Subsystem	Component/Specification
Control	ESP32 development board
Motor driver	L298N dual H-bridge module
Power supply	3S LiPo battery, 11.1 V, 2200 mAh
Voltage regulation	LM2596 DC-DC buck converter
Locomotion	Low-speed, high-torque DC geared motors
Cleaning motor	TT DC geared motor, 3 - 6 V
Cleaning tools	Cylindrical brush; circular disc brush; 6 V blower fan
Edge sensing	KY-032 infrared sensor; HC-SR04 ultrasonic sensor

2.2. Autonomous Control Strategy

The operational sequence was implemented in the ESP32. When the start button was activated, the controller initialized the motor driver, edge-detection sensor, and cleaning subsystem. The robot then travelled forward while the rotating brush

and blower operated continuously. During operation, the edge-detection sensor continuously monitored the panel boundary. Once an edge was detected, the robot stopped, reversed by a short distance, and performed a box-turn manoeuvre consisting of two approximately 90˚ turns separated by a short forward movement. This repositioned the robot into the next cleaning lane, as illustrated in Figure 3(a).

A raster or zig-zag cleaning strategy was selected to provide systematic coverage of the rectangular panel surface, as shown in Figure 3(b). Similar path-planning approaches have been investigated for photovoltaic cleaning robots to reduce uncleaned regions and improve navigation efficiency [17]. The required number of cleaning passes was predetermined according to the available panel width and effective cleaning width. Each edge-detection event represented the completion of one cleaning lane, allowing the controller to track cleaning progress. After the final lane was completed, the system stopped automatically. An emergency-stop button was continuously monitored and immediately disabled the locomotion motors, cleaning brush, and blower when activated.

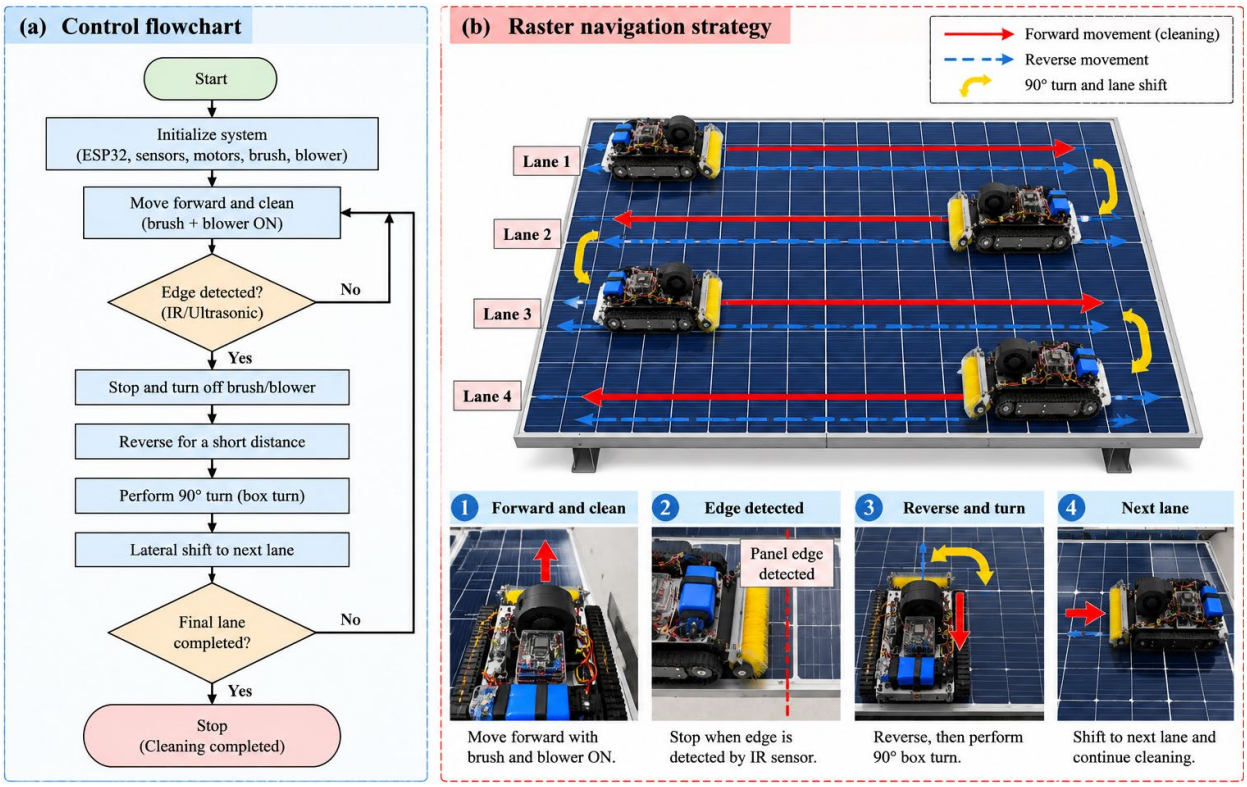


Figure 3. Autonomous cleaning control and navigation strategy: (a) Control flowchart of the robot operating sequence; (b) Raster navigation strategy showing forward cleaning, edge detection, reverse and box-turn manoeuvre, and movement to the next cleaning lane.

2.3. Experimental Evaluation

Three comparative experiments were conducted under controlled laboratory conditions (see Figure 4). The experiments were designed to maintain equivalent in-

itial conditions between competing configurations, with seven repeated runs performed for each test condition.

Experiment 1 evaluated sensor reliability for panel-edge detection. The infrared KY-032 and ultrasonic HC-SR04 sensors were mounted at identical positions and orientations on the robot chassis. At the beginning of each trial, the robot was positioned 1.0 m from the panel edge and commanded to travel forward at a constant speed. Timing stopped when the respective sensor generated an edge-detection event. The recorded parameters were successful edge detection and motion-to-detection time. Note that the measurement includes travel time. The actual travel speed and sensor trigger distance were not independently recorded during the original experiments; therefore, the reported motion-to-detection time should not be interpreted as intrinsic sensor response latency. Detection accuracy and miss rate were calculated as:

$$\text{Detection Accuracy}(\%) = \frac{N_{\text{successful}}}{N_{\text{total}}} \times 100 \tag{1}$$

$$\text{Miss Rate}(\%) = \frac{N_{\text{missed}}}{N_{\text{total}}} \times 100 \tag{2}$$

where $N_{\text{successful}}$ is the number of successful detections, N_{missed} is the number of missed detections, and N_{total} is the total number of trials. Mean motion-to-detection time was calculated using the successful detection trials.

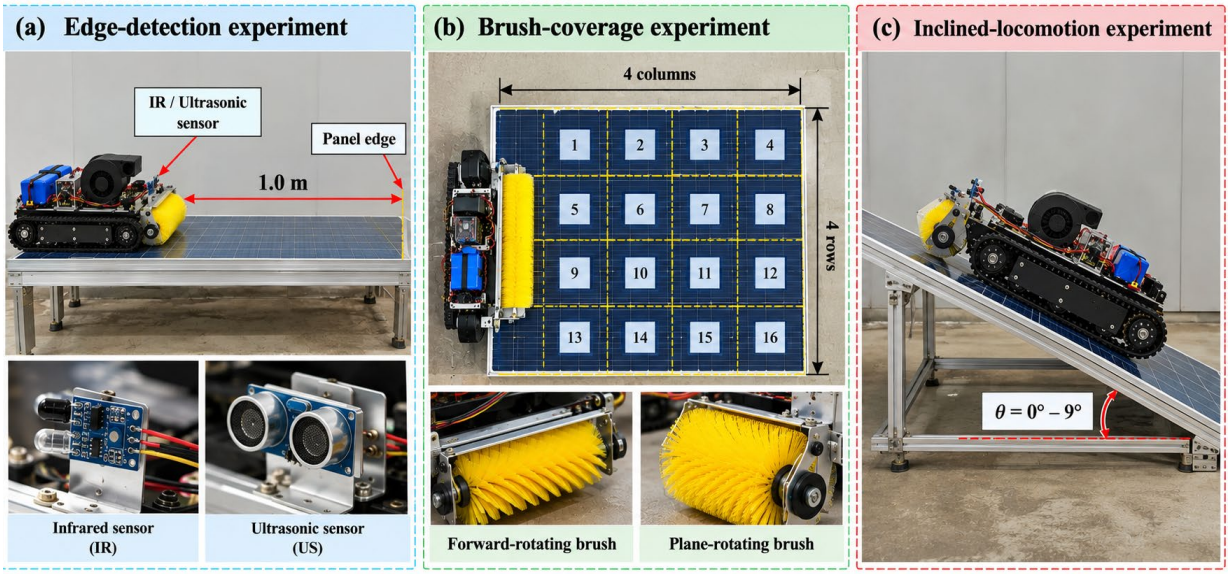


Figure 4. Experimental arrangements: (a) Edge-detection test; (b) Brush-coverage test using a 4 × 4 grid; (c) Locomotion test at different inclination angles.

Experiment 2 examined the effectiveness of the cleaning mechanism. Two nylon-brush configurations were compared: a forward-rotating cylindrical brush and a plane-rotating circular brush. The test surface was divided into a 4 × 4 grid consisting of 16 equal cells. Before each trial, a fresh dust layer was applied as

uniformly as practicable over the test area. To provide a consistent basis for comparison, both brush configurations were operated using the same motor-control setting and nominal contact condition, while the inspection procedure, lighting, and viewing conditions were kept unchanged. However, the dust composition and areal loading, brush rotational speed, brush dimensions, and applied contact force were not independently quantified during the original experiments. These variables were therefore controlled by maintaining the same experimental procedure between configurations rather than by direct measurement. Blower operation was not independently characterized as part of the brush-comparison experiment and was therefore not treated as a quantified experimental variable. Each brush configuration was tested over seven repeated trials, with the dust layer reapplied before every trial.

Cleaning performance was evaluated using the cleaning coverage, *Cov*, mean residue, and coefficient of variation, *CV*. Cleaning coverage represents the proportion of grid cells classified as clean after each trial and was calculated as:

$$Cov(\%) = \frac{C}{16} \times 100 \tag{3}$$

where C is the number of clean cells out of the 16 grid cells.

The mean coverage and mean residue were then determined across the seven repeated trials. The coefficient of variation, *CV*, was used to evaluate the consistency of cleaning performance between trials, with a lower CV indicating lower run-to-run variability. It was calculated as:

$$CV(\%) = \frac{\sigma}{\mu} \times 100 \tag{4}$$

where σ represents the standard deviation of coverage and μ is the corresponding mean coverage.

Experiment 3 evaluated locomotion reliability on inclined PV surfaces. Wheel-based and track-based drivetrains were tested under equivalent mass, power supply, and motor-control conditions. The panel inclination was varied between 0˚, 3˚, 6˚, and 9˚. For each drivetrain and inclination combination, the robot travelled along a fixed straight path at a constant target speed, and seven consecutive trials were conducted. Traversal time was recorded for each run, and the mean traversal time and sample standard deviation were subsequently calculated to compare mobility performance and run-to-run consistency.

Statistical analysis was performed using the repeated-trial data from the three experiments. The seven runs for each configuration were treated as independent repeated trials because the experimental design did not employ matched trial pairs. Detection success rates were reported with exact 95% binomial confidence intervals (CI). For continuous performance measures, 95% CIs for the mean were calculated using the Student's *t*-distribution. Differences between alternative configurations were evaluated using 95% CIs based on independent-sample Welch estimates, which do not assume equal variances. Given the exploratory nature of the study and the small number of trials, the confidence intervals were used primarily

to indicate the uncertainty and magnitude of the observed differences.

The comparative results from these three experiments were then used to determine the components incorporated into the final autonomous cleaning prototype. In this manner, the final configuration was selected on the basis of experimental performance rather than component specification alone.

3. Results and Discussion

The performance of the autonomous solar panel cleaning robot was evaluated through three comparative experiments involving edge detection, cleaning coverage, and locomotion on inclined surfaces. The results from each experiment were used to identify the most suitable configuration for integration into the final prototype.

3.1. Edge Detection Performance

The performance of the infrared (IR) and ultrasonic sensors was first evaluated for reliable detection of the solar panel edge. Table 2 summarizes the results obtained over seven repeated trials. The infrared sensor detected the panel edge in all seven trials, corresponding to an observed success rate of 100%; however, the exact 95% CI was 59.0% - 100.0%, reflecting the uncertainty associated with the small sample size. The ultrasonic sensor detected the edge in five of seven trials, corresponding to 71.4% with a 95% CI of 29.0% - 96.3%. The mean motion-to-detection time was 5.09 s (95% CI: 5.01 - 5.16 s) for the infrared sensor and 5.39 s (95% CI: 5.27 - 5.50 s) for the successful ultrasonic trials. Therefore, although the infrared sensor showed a higher observed detection success rate under the tested conditions, the limited number of trials means that its reliability should be regarded as preliminary rather than definitive.

Table 2. Sensor reliability test results.

Sensor	Detection Success	Detection Accuracy (%)	Exact 95% CI (%)	Mean Motion-to-Detection Time (s)	95% CI (s)
Infrared	7/7	100	59 - 100	5.09	5.01 - 5.16
Ultrasonic	5/7	71.43	29 - 96.3	5.39*	5.27 - 5.50

Note: *Calculated from the five successful ultrasonic detections.

In comparison, the ultrasonic sensor successfully detected the edge in only five of the seven trials, resulting in an accuracy of 71.43% and a miss rate of 28.57%. For the successful trials, the time from motion start to edge detection ranged from 5.28 s to 5.50 s, with a mean of 5.39 s. One possible explanation for the missed ultrasonic detections is weak or incomplete acoustic reflection from the smooth panel boundary. However, the reflected acoustic signal was not independently measured during the experiment; therefore, this mechanism cannot be confirmed directly from the present data.

The observed difference is noteworthy because ultrasonic sensing has been successfully employed for localization and trajectory adjustment in previous solar-cleaning robots [9] [11]. However, such sensing depends on the quality of the reflected acoustic signal and therefore remains sensitive to target geometry and sensor positioning. Under the smooth-surface and boundary conditions used in this study, the infrared sensor provided more repeatable edge detection. This result does not imply that infrared sensing is universally superior to ultrasonic sensing, but demonstrates its suitability for the specific lightweight prototype evaluated here. More sophisticated systems may employ vision and sensor-fusion approaches when higher localization accuracy is required [16].

3.2. Cleaning Coverage Performance

The second experiment compared a forward-rotating cylindrical brush with a plane-rotating circular brush. Cleaning coverage was evaluated using the number of clean cells within the 4 × 4 test grid after each cleaning pass. Table 3 summarizes the performance of both brush configurations over seven trials. The plane-rotating brush produced a mean coverage improvement of 13.4 percentage points relative to the forward-rotating brush (95% CI: 8.7 - 18.0 percentage points).

Table 3. Brush cleaning coverage results.

Brush Configuration	Mean Coverage, Cov (%)	95% CI (%)	Mean Residue (%)	CV (%)
Forward-rotating	61.6	57.6 - 65.6	38.4	7
Plane-rotating	75	71.7 - 78.3	25	4.8

For the forward-rotating brush, the number of clean cells varied between 9 and 11 cells out of 16, corresponding to a mean cleaning coverage of 61.6%. Approximately 38.4% of the test surface therefore remained uncleaned after a single pass. The CV was 7.0%, indicating moderate run-to-run variation. Inspection of the test surface showed that the remaining dust tended to accumulate along one side of the cleaning path. This behaviour was associated with the directional sweeping action of the cylindrical brush, in which linear brush contact displaced dust predominantly in one direction.

The plane-rotating brush produced higher overall cleaning coverage. The number of clean cells ranged from 11 to 13 out of 16 during the seven runs, resulting in an average coverage of 75.0% and average residue of 25.0%. The corresponding CV of 4.8% was lower than that obtained for the forward-rotating brush, indicating more consistent cleaning performance between repeated trials. The remaining residue was concentrated mainly at the corners of the square grid, reflecting the circular cleaning profile operating over a square test region.

The advantage of the plane-rotating configuration is consistent with the broader use of mechanical brushing in dry-cleaning PV robots. Parrott *et al.* [7] demonstrated that robotic dry cleaning using a compliant brush could mitigate dust-re-

lated performance losses without measurable panel damage, while Amin *et al.* [12] demonstrated the feasibility of automated dry-cleaning combined with panel-condition monitoring. Other autonomous platforms have similarly used rotating or helical brush arrangements for water-free dust removal [9]. Automated cleaning-machine studies also support mechanical brushing as a practical PV maintenance approach [18]. The present results additionally show that brush orientation and contact geometry influence the spatial coverage obtained during a single pass. Because the corner residue of the plane-rotating brush can potentially be reduced through overlapping passes, this configuration was selected for the final prototype.

3.3. Locomotion Performance on Inclined Surfaces

The third experiment evaluated the ability of wheel-based and track-based drivetrains to maintain consistent movement as the inclination of the PV surface increased. Each drivetrain was tested seven times at inclination angles of 0˚, 3˚, 6˚, and 9˚. The resulting mean traversal times and standard deviations are presented in **Table 4**.

Table 4. Locomotion reliability test results.

Drivetrain	Inclination Angle (˚)	Mean Time (s)	Standard Deviation (s)	95% CI for Mean (s)
Wheel-based	0	5.06	0.08	4.98 - 5.13
	3	5.31	0.11	5.22 - 5.41
	6	6.10	0.22	5.90 - 6.30
	9	7.96	0.46	7.53 - 8.38
Track-based	0	5.44	0.10	5.35 - 5.53
	3	5.50	0.08	5.42 - 5.58
	6	5.69	0.09	5.60 - 5.77
	9	5.97	0.11	5.87 - 6.07

The wheel-based drivetrain exhibited slightly faster movement on the horizontal surface, recording a mean traversal time of 5.06 s compared with 5.44 s for the track-based system. However, its performance progressively deteriorated as the inclination increased. Mean traversal time rose to 5.31 s at 3˚, 6.10 s at 6˚, and 7.96 s at 9˚. At the same time, the standard deviation increased from 0.08 s at 0˚ to 0.46 s at 9˚, indicating decreasing repeatability. As illustrated in **Figure 5**, the wheel-based drivetrain showed a pronounced upward trend in traversal time as the panel inclination increased, together with progressively larger error bars at the higher inclination angles. The increasing traversal time and variability at higher inclination angles may indicate reduced traction or intermittent wheel slip. However, wheel slip was not independently measured during the experiment; therefore, it should be regarded as a possible explanation rather than a directly verified failure mechanism.

In contrast, the track-based drivetrain showed only a small increase in traversal time over the same inclination range. Mean time increased from 5.44 s at 0˚ to 5.50 s at 3˚, 5.69 s at 6˚, and 5.97 s at 9˚. Standard deviations remained between 0.08 s and 0.11 s, indicating that repeatability was largely maintained as the panel angle increased. Figure 5 shows that the track-based drivetrain maintained a comparatively flat traversal-time profile with consistently small error bars across the tested inclination range, indicating lower sensitivity to increasing panel angle.

Independent-sample comparisons showed that the wheel-based drivetrain was faster at 0˚ and 3˚, whereas the track-based drivetrain became faster at steeper inclinations. At 6˚, the track-based drivetrain was faster by 0.41 s (95% CI: 0.21 - 0.62 s), while at 9˚ it was faster by 1.99 s (95% CI: 1.56 - 2.41 s). These results indicate that the performance advantage of the track-based drivetrain became more pronounced as inclination increased.

The observed stability of the track-based drivetrain may be partly attributed to its larger contact area and more distributed surface loading, which are commonly associated with improved traction in tracked systems. Yang *et al.* [14] similarly noted that track-wheel arrangements can increase contact area and available traction in photovoltaic cleaning applications, while tracked or partially tracked configurations are commonly adopted in autonomous PV cleaning systems [9] [13]. The present results extend these observations by quantitatively comparing wheel- and track-based configurations under the same prototype mass, power-supply, and control conditions. Consequently, the track-based drivetrain was selected for the final prototype.

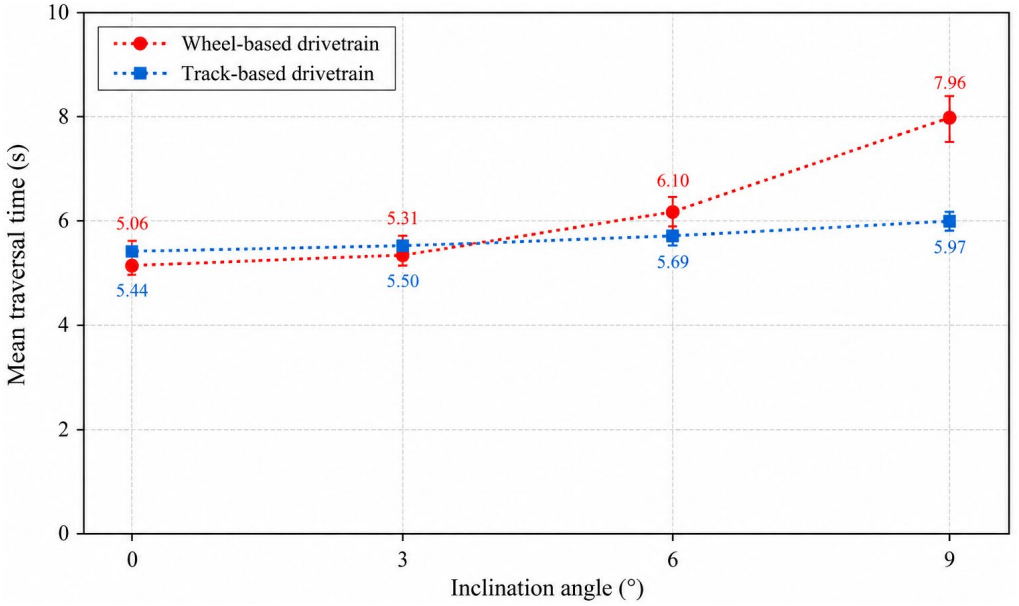


Figure 5. Effect of panel inclination on the mean traversal time of wheel-based and track-based drivetrains.

3.4. Overall Prototype Performance

Based on the comparative experiments, the final prototype incorporated the in-

frared edge-detection sensor, plane-rotating brush with blower, and track-based drivetrain. The completed robot measured approximately 350 mm in length, 210 mm in width, and 130 mm in height, with a total assembled mass of approximately 1.3 kg.

The three selected subsystems addressed different requirements of autonomous operation. The infrared sensor detected the panel edge successfully in all seven experimental trials; however, the small sample size limits the precision of the reliability estimate. The plane-rotating brush provided a mean cleaning coverage of 75.0% with a CV of 4.8%, while the track-based drivetrain maintained mean traversal times between 5.44 s and 5.97 s from 0˚ to 9˚ inclination with low standard deviations. Following integration, the robot performed the intended autonomous operating sequence, including forward movement, edge detection, stopping, turning, lane alignment, and continuous activation of the dry-cleaning mechanism.

The integrated configuration represents a compromise between sensing reliability, cleaning coverage, and inclined locomotion rather than maximizing a single performance variable. This subsystem-oriented approach is consistent with reviews that identify cleaning, locomotion, navigation, and control as interdependent design considerations in solar-panel cleaning robots [13]. Compared with systems incorporating more complex localization [16] or IoT-based monitoring [15], the present prototype emphasizes a relatively simple embedded architecture suitable for proof-of-concept autonomous cleaning.

The results should nevertheless be interpreted within the experimental conditions used in this study. The brush experiment was performed using a controlled grid and one dust condition, while locomotion was evaluated only up to a 9˚ inclination. The experiments were conducted under controlled conditions rather than extended outdoor operation. Outdoor validation remains necessary because dust adhesion and cleaning effectiveness depend strongly on dust properties, humidity, wind, rainfall, and other environmental conditions [2]-[5]. Furthermore, practical cleaning frequency should ultimately be determined according to local soiling rates and economic considerations rather than by a fixed schedule [19] [20].

4. Conclusions

This study presented the design, development, and experimental evaluation of an autonomous dry-cleaning robot for photovoltaic panel maintenance. The system integrated an ESP32-based controller with edge detection, a mechanical brush-and-blower cleaning mechanism, and an interchangeable locomotion platform. Three comparative experiments were conducted to identify suitable sensing, cleaning, and drivetrain configurations for the final prototype.

The infrared sensor successfully detected the panel edge in all seven trials, corresponding to an observed detection rate of 100%, although the wide 95% confidence interval reflects the uncertainty associated with the limited number of repetitions. The ultrasonic sensor, in comparison, achieved an observed detection rate

of 71.43% (5/7 successful detections). Based on the higher observed detection success under the tested laboratory conditions, the infrared sensor was selected for autonomous boundary detection. The plane-rotating brush achieved an average cleaning coverage of 75.0%, with 25.0% residue and a CV of 4.8%, outperforming the forward-rotating cylindrical brush, which achieved 61.6% coverage.

Based on these results, the final prototype incorporated the infrared sensor, plane-rotating brush with blower, and track-based drivetrain. The integrated system was able to perform the intended autonomous functions, including forward movement, edge detection, stopping, turning, lane alignment, and continuous dry cleaning. These findings demonstrate the feasibility of combining sensing, cleaning, and locomotion subsystems in a compact water-free solar panel maintenance platform under controlled experimental conditions.

Nevertheless, the prototype remains at the proof-of-concept stage. Further work should include testing at steeper panel angles, outdoor operation on naturally soiled PV modules, evaluation under different dust and environmental conditions, measurement of PV electrical-performance recovery before and after cleaning, and long-term durability testing of the brush, motors, and track system. With further field validation, autonomous dry cleaning could contribute to water-efficient photovoltaic maintenance and reduce the operational burden associated with recurrent soiling [5] [19].

Acknowledgements

The authors would like to thank Universiti Teknikal Malaysia Melaka (UTeM), particularly the Faculty of Electrical Technology and Engineering, for providing the facilities and financial support required to complete this study.

Author Contributions

Mohd Rusdy Yaacob: Conceptualization, methodology, supervision, validation, and writing. Anuar Mohamed Kassim: Methodology, supervision, validation, and writing. Nik Nurqairina Eriza Nik Ahmad Yusri: Investigation, experimental work, data collection, data analysis, visualization, and writing. All authors have read and agreed to the published version of the manuscript.

Conflicts of Interest

The authors declare no conflicts of interest regarding the publication of this paper.

References

[1] Maghami, M.R., Hizam, H., Gomes, C., Radzi, M.A., Rezadad, M.I. and Hajighorbani, S. (2016) Power Loss Due to Soiling on Solar Panel: A Review. *Renewable and Sustainable Energy Reviews*, **59**, 1307-1316. https://doi.org/10.1016/j.rser.2016.01.044

[2] Ilse, K.K., Figgis, B.W., Naumann, V., Hagendorf, C. and Bagdahn, J. (2018) Fundamentals of Soiling Processes on Photovoltaic Modules. *Renewable and Sustainable Energy Reviews*, **98**, 239-254. https://doi.org/10.1016/j.rser.2018.09.015

[3] Gupta, V., Sharma, M., Pachauri, R.K. and Dinesh Babu, K.N. (2019) Comprehensive

Review on Effect of Dust on Solar Photovoltaic System and Mitigation Techniques. *Solar Energy*, **191**, 596-622. https://doi.org/10.1016/j.solener.2019.08.079

[4] Salamah, T., Ramahi, A., Alamara, K., Juaidi, A., Abdallah, R., Abdelkareem, M.A., *et al.* (2022) Effect of Dust and Methods of Cleaning on the Performance of Solar PV Module for Different Climate Regions: Comprehensive Review. *Science of the Total Environment*, **827**, Article ID: 154050. https://doi.org/10.1016/j.scitotenv.2022.154050

[5] Najmi, N. and Rachid, A. (2023) A Review on Solar Panel Cleaning Systems and Techniques. *Energies*, **16**, Article No. 7960. https://doi.org/10.3390/en16247960

[6] Kawamoto, H. and Shibata, T. (2015) Electrostatic Cleaning System for Removal of Sand from Solar Panels. *Journal of Electrostatics*, **73**, 65-70. https://doi.org/10.1016/j.elstat.2014.10.011

[7] Parrott, B., Carrasco Zanini, P., Shehri, A., Kotsovos, K. and Gereige, I. (2018) Automated, Robotic Dry-Cleaning of Solar Panels in Thuwal, Saudi Arabia Using a Silicone Rubber Brush. *Solar Energy*, **171**, 526-533. https://doi.org/10.1016/j.solener.2018.06.104

[8] Riawan, I.P.G., Kumara, I.N.S., Partha, C.G.I., Setiawan, I.N. and Santiari, D.A.S. (2018) Robot for Cleaning Solar PV Module to Support Rooftop PV Development. 2018 *International Conference on Smart Green Technology in Electrical and Information Systems* (*ICSGTEIS*), Bali, 25-27 October 2018, 132-137. https://doi.org/10.1109/icsgteis.2018.8709138

[9] Antonelli, M.G., Beomonte Zobel, P., De Marcellis, A. and Palange, E. (2020) Autonomous Robot for Cleaning Photovoltaic Panels in Desert Zones. *Mechatronics*, **68**, Article ID: 102372. https://doi.org/10.1016/j.mechatronics.2020.102372

[10] Salman, M.H., Abid, A.J. and Obed, A.A. (2021) Robotic Dry Cleaner for Photovoltaic Solar Panels: An Implemented Design That Evaluated in Iraq's Weather. *TELKOMNIKA* (*Telecommunication Computing Electronics and Control*), **19**, 2050-2058. https://doi.org/10.12928/telkomnika.v19i6.20505

[11] Mousavi, S. and Farahani, G. (2022) Introducing a New Method of Automatic Cleaning of the PV Array Surface Using a Suction Robot. *Mechatronics*, **85**, Article ID: 102845. https://doi.org/10.1016/j.mechatronics.2022.102845

[12] Amin, A., Wang, X., Alroichdi, A. and Ibrahim, A. (2023) Designing and Manufacturing a Robot for Dry-Cleaning PV Solar Panels. *International Journal of Energy Research*, **2023**, Article ID: 7231554. https://doi.org/10.1155/2023/7231554

[13] Sarode, N., Ghugal, P., Yadav, S., Dantule, S. and Nandankar, P. (2023) A Comprehensive Review on Solar Panel Cleaning Robot Technologies. *AIP Conference Proceedings*, **2753**, Article ID: 020018. https://doi.org/10.1063/5.0127800

[14] Yang, J., Zhao, X., Gao, Y., Guo, R. and Zhao, J. (2023) Research on Mechanism Design and Kinematic Characteristics of Self-Propelled Photovoltaic Cleaning Robot. *Applied Sciences*, **13**, Article No. 6967. https://doi.org/10.3390/app13126967

[15] Biswas, S., Bhuyan, M.H. and Hassan, M.K. (2023) IoT-Based Automated Solar Panel Cleaning and Monitoring Technique. *Journal of Engineering Research and Reports*, **25**, 56-69. https://doi.org/10.9734/jerr/2023/v25i8959

[16] Kim, J.H., Lee, S.H., Kim, J.G., Jang, W.J. and Kim, D.H. (2024) Localization of Solar Panel Cleaning Robot Combining Vision Processing and Extended Kalman Filter. *Science Progress*, **107**, 1-29. https://doi.org/10.1177/00368504241250176

[17] Jin, L.-W., Meng, G.-S., Zheng, H.-L., *et al.* (2024) Design and Path Planning Method of Control System for Photovoltaic Panel Cleaning Robot. *Journal of Computers*, **35**,

175-190. https://doi.org/10.53106/199115992024083504013

[18] Patil, S.A., Patil, A.R., Chougule, V.N. and Sanamdikar, S.T. (2024) Design and Analysis of Automated Solar Panel Cleaning System. *Current World Environment*, **18**, 1032-1045. https://doi.org/10.12944/cwe.18.3.11

[19] Azouzoute, A., Zitouni, H., El Ydrissi, M., Hajjaj, C., Garoum, M., Bennouna, E.G., *et al.* (2021) Developing a Cleaning Strategy for Hybrid Solar Plants PV/CSP: Case Study for Semi-Arid Climate. *Energy*, **228**, Article ID: 120565. https://doi.org/10.1016/j.energy.2021.120565

[20] Naeem, M. and TamizhMani, G. (2015) Cleaning Frequency Optimization for Soiled Photovoltaic Modules. 2015 *IEEE* 42*nd Photovoltaic Specialist Conference* (*PVSC*), New Orleans, 14-19 June 2015, Article ID: 7355972. https://doi.org/10.1109/pvsc.2015.7355972